High Frequency Spin Torque Oscillation in Orthogonal Magnetization Disks with Strong Biquadratic Magnetic Coupling

*C. Liu, Y. Kurokawa, N. Hashimoto, T. Tanaka and †H. Yuasa

Graduate School and Faculty of Information Science and Electrical Engineering Kyushu University, Fukuoka 819-0395, Japan

*E-mail: *liu@mag.kyushu-u.ac.jp, †hiromi.yuasa@ed.kyushu-u.ac.jp

In order to confirm the current density limit realizing the stable magnetization oscillation, we calculated the STO properties with systematically and widely changing the current density for the top layer $Co_{90}Fe_{10}$, $Ni_{80}Fe_{20}$, and Ni in the orthogonal configuration where the initial state is out of plane (z-axis) and in-plane (y-axis). As well as Fig. 2 and Fig. 4, the time-domain magnetization precessions M_x/M_s, the Fast Fourier transform spectra, and side views of magnetization configuration are shown. Light blue and orange plot denotes the result for B_{12}=0.0 and B_{12}=−0.6.

Table S1 Calculation conditions in Fig. S1-S6.

Fig.	Top layer	Magnetization in initial state	Current density
S1	$Co_{90}Fe_{10}$	out of plane (z axis)	8.0×10^7 A/cm^2 ~ 20.0×10^7 A/cm^2
S2	$Ni_{80}Fe_{20}$	out of plane (z axis)	0.5×10^7 A/cm^2 ~ 6.0×10^7 A/cm^2
S3	Ni	out of plane (z axis)	0.5×10^7 A/cm^2 ~ 6.0×10^7 A/cm^2
S4	$Co_{90}Fe_{10}$	in-plane (y axis)	8.0×10^7 A/cm^2 ~20.0×10^7 A/cm^2
S5	$Ni_{80}Fe_{20}$	in-plane (y axis)	0.5×10^7 A/cm^2 ~ 6.0×10^7 A/cm^2
S6	Ni	in-plane (y axis)	0.5×10^7 A/cm^2 ~ 6.0×10^7 A/cm^2

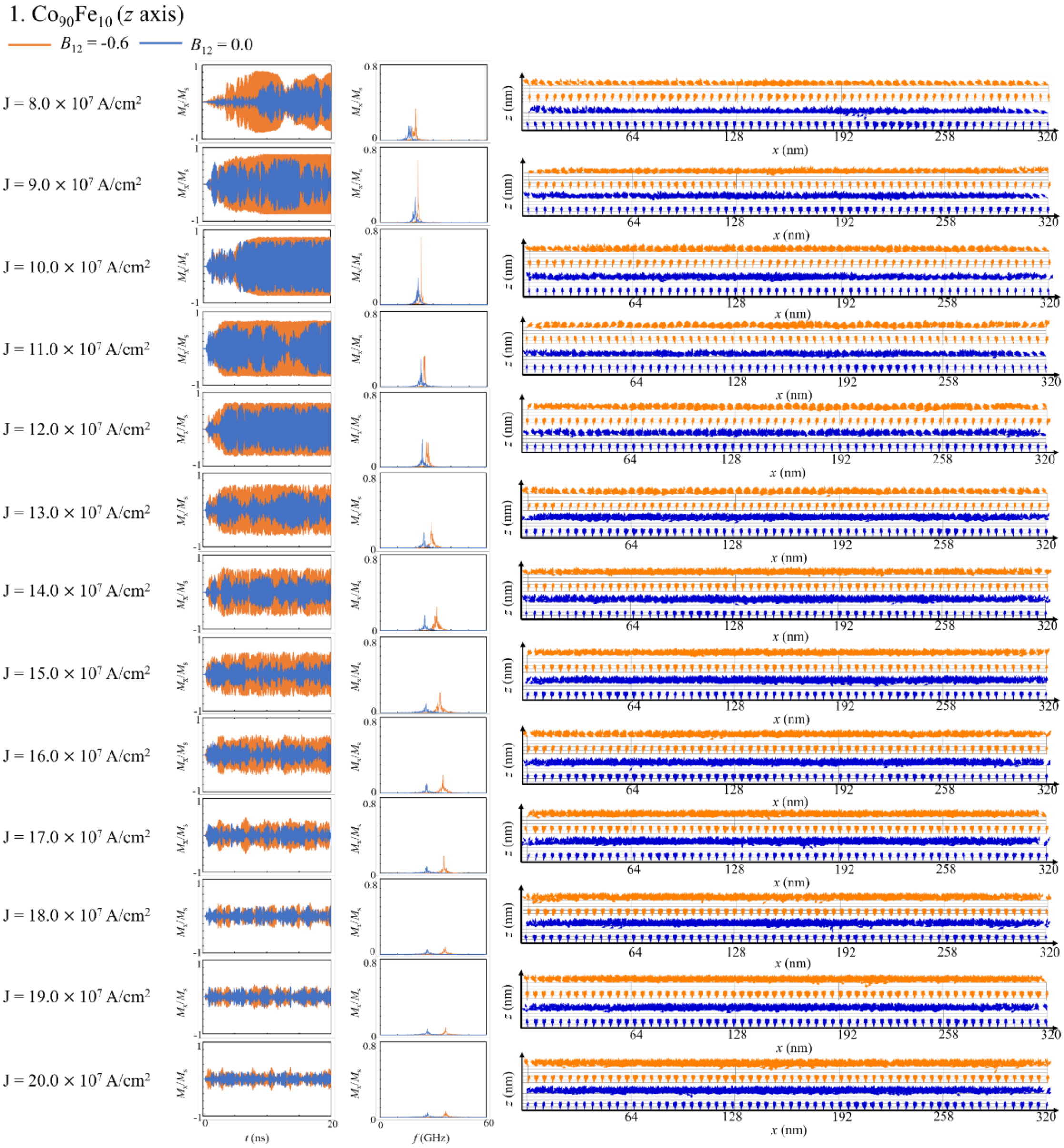

Fig. S1 STO performances for the top layer $Co_{90}Fe_{10}$ in the orthogonal configuration where the initial state is out of plane, namely *z*-axis. The electrical current density was varied from 8×10^7 A/cm^2 to 20×10^7 A/cm^2.

2. $Ni_{80}Fe_{20}$ (*z* axis)

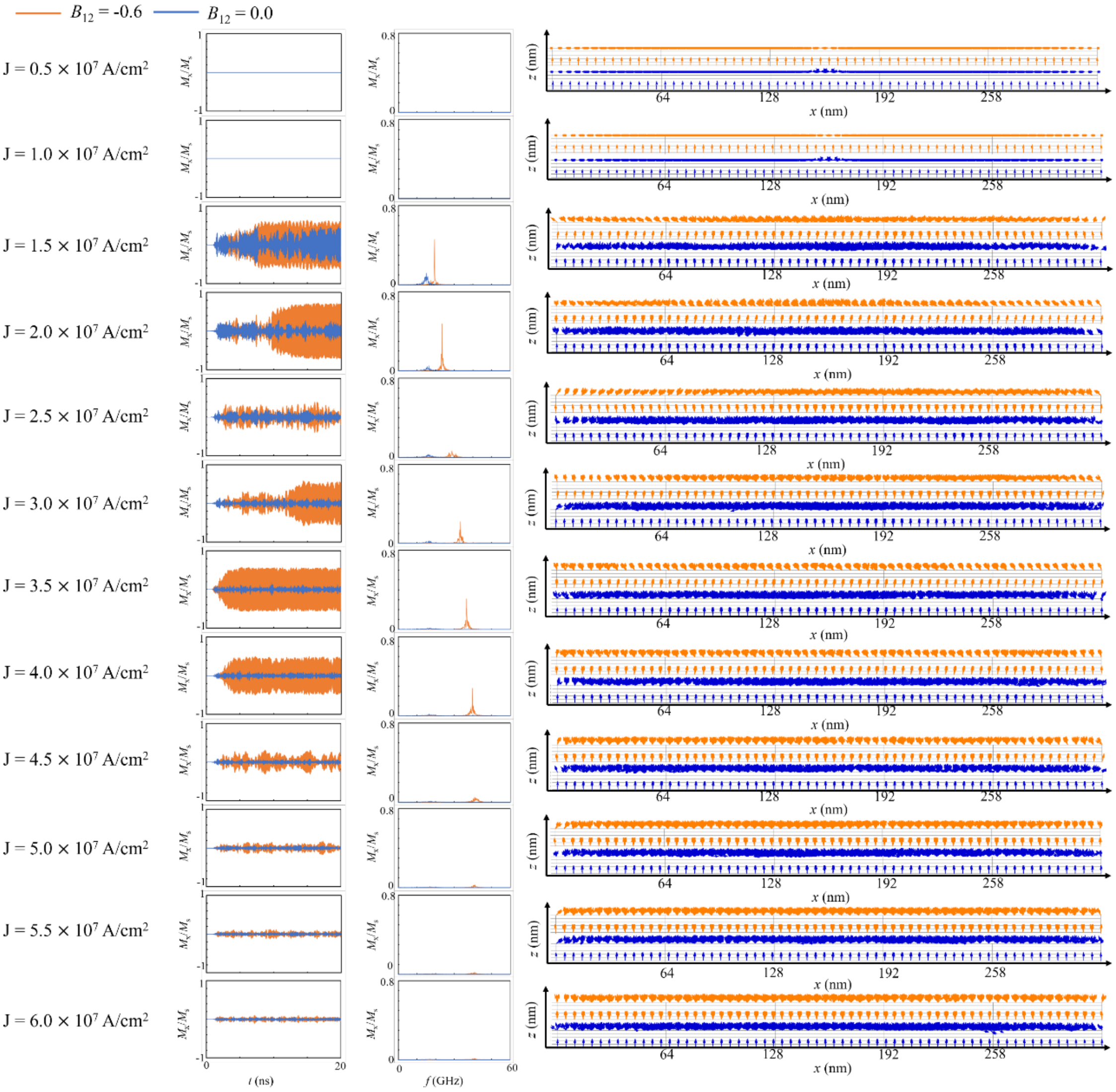

Fig. S2 STO performances for the top layer $Ni_{80}Fe_{20}$ in the orthogonal configuration where the initial state is out of plane, namely *z*-axis. The electrical current density was varied from 0.5×10^7 A/cm^2 to 6.0×10^7 A/cm^2.

3. Ni (*z* axis)

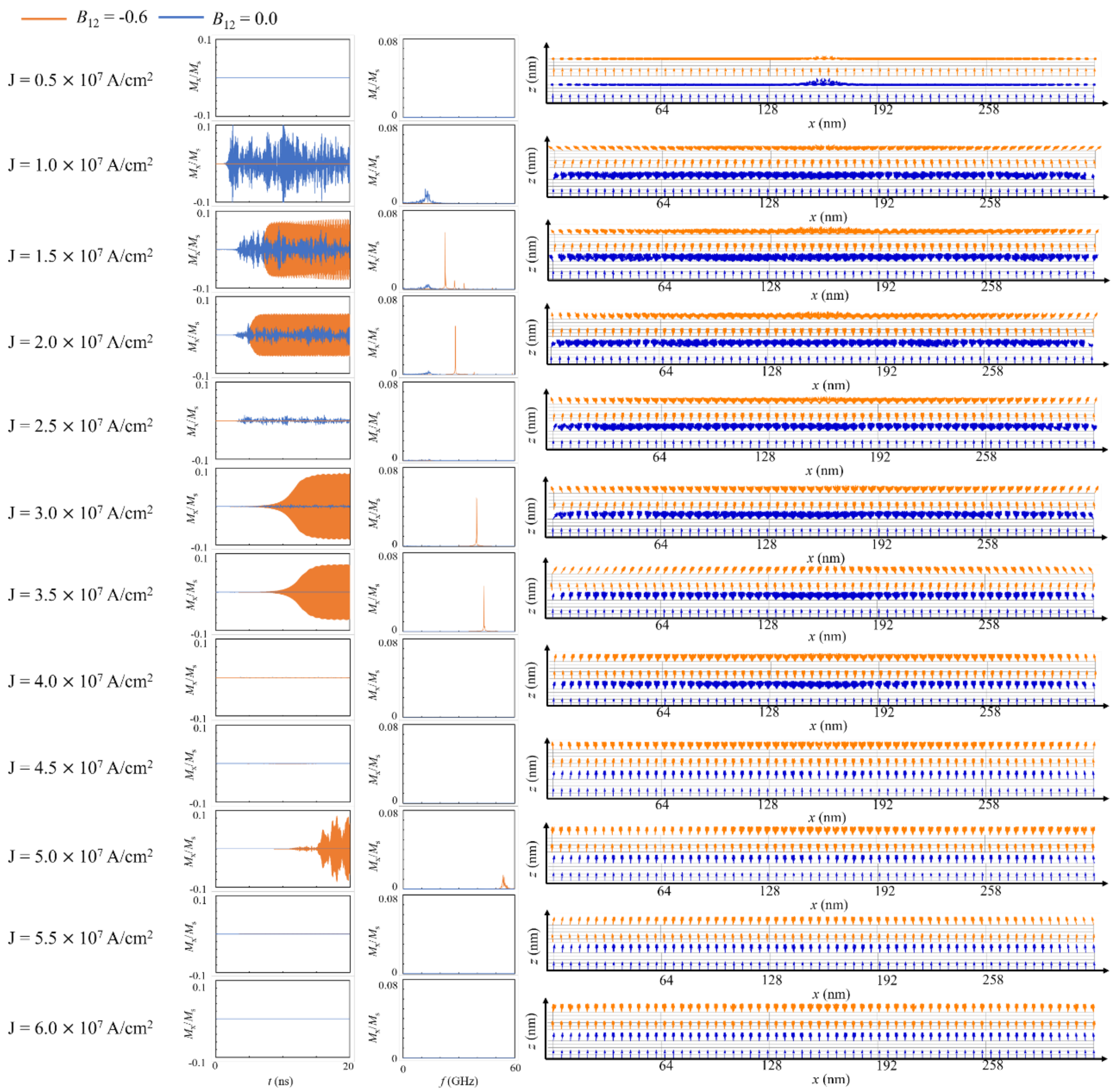

Fig. S3 STO performances for the top layer Ni in the orthogonal configuration where the initial state is out of plane, namely *z*-axis. The electrical current density was varied from 0.5×10^7 A/cm^2 to 6.0×10^7 A/cm^2.

4. $Co_{90}Fe_{10}$ (*y* axis)

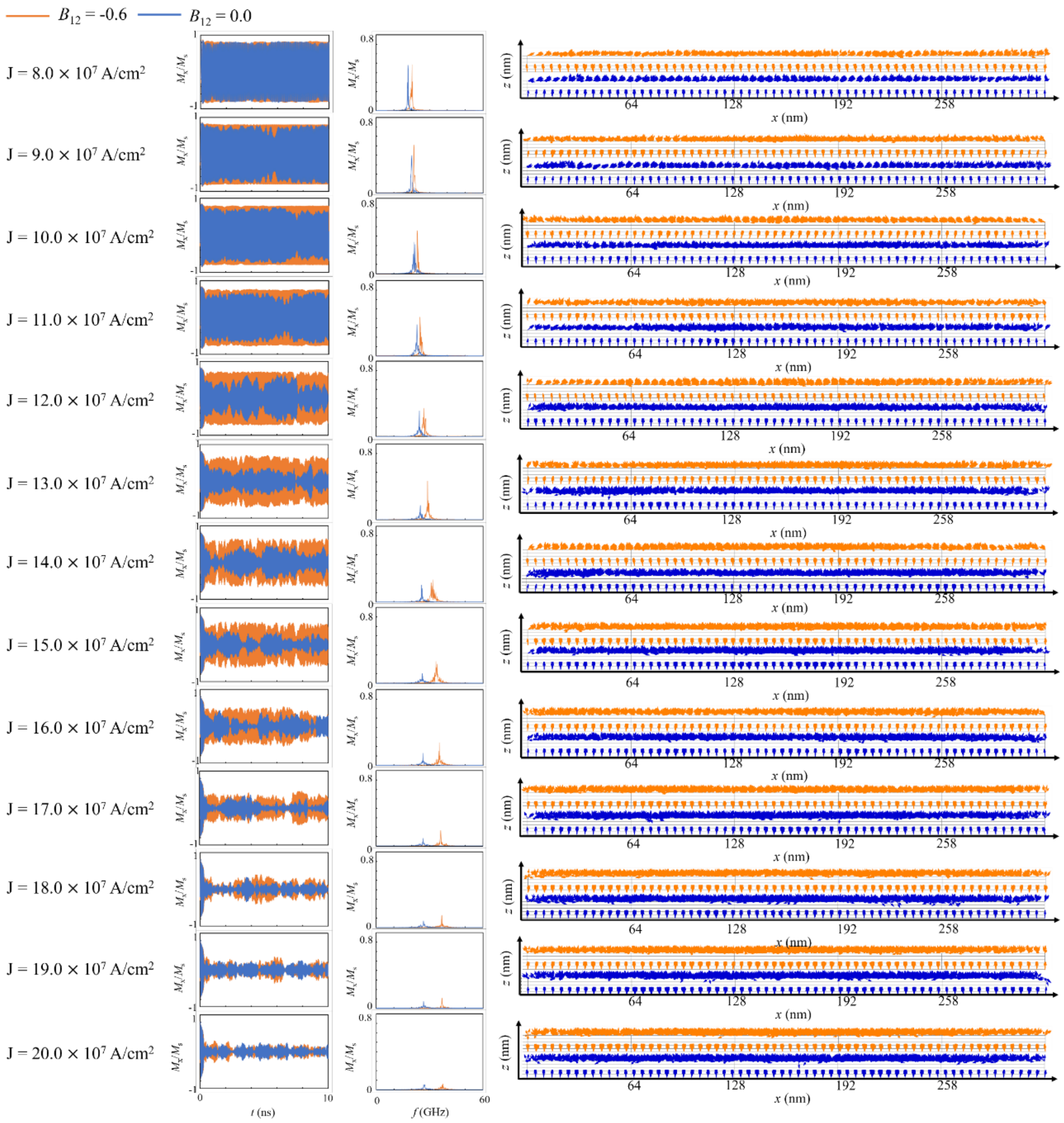

Fig. S4 STO performances for the top layer $Co_{90}Fe_{10}$ in the orthogonal configuration where the initial state is in- plane, namely *y*-axis. The electrical current density was varied from 8×10^7 A/cm^2 to 20×10^7 A/cm^2.

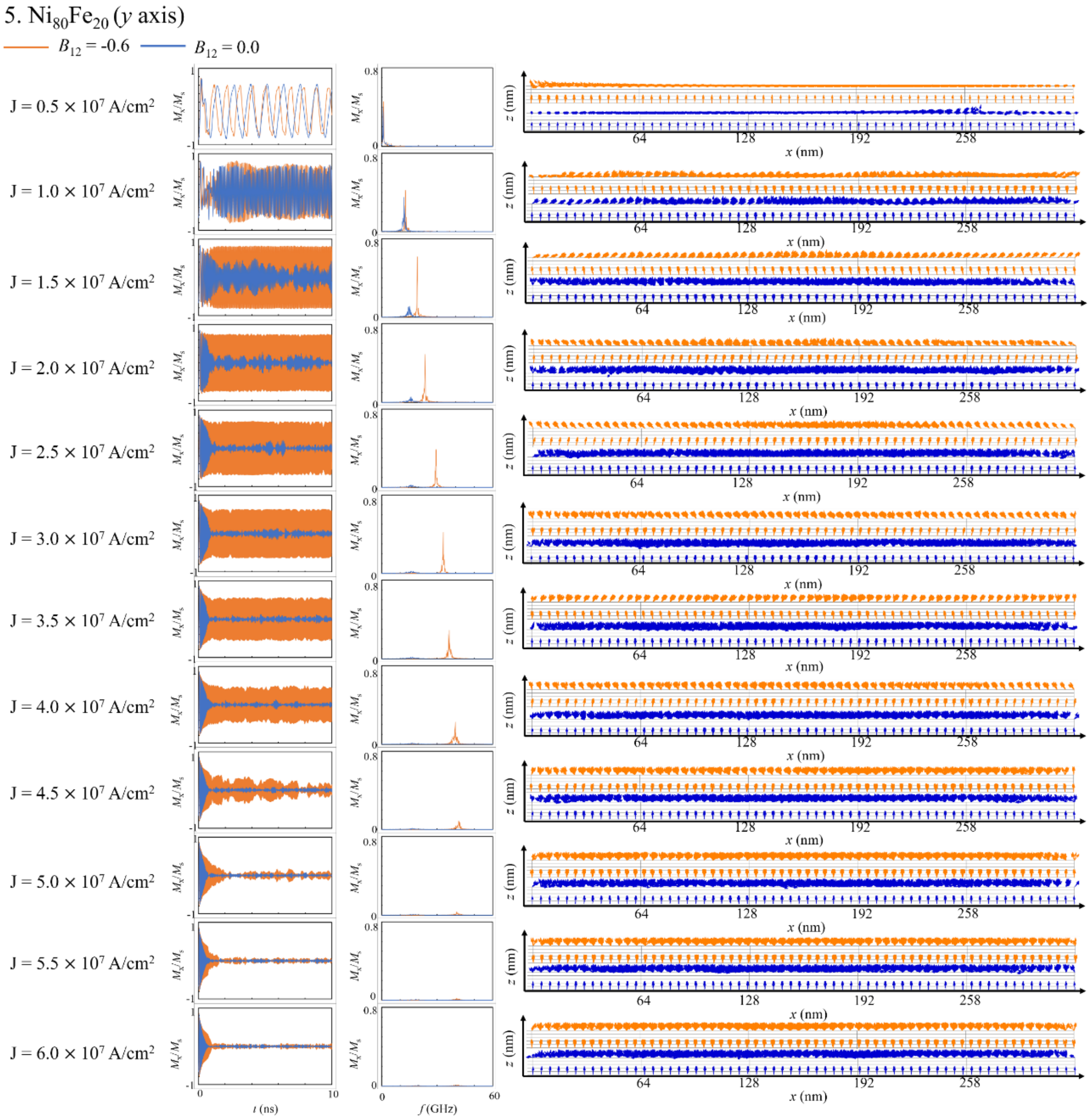

Fig. S5 STO performances for the top layer $Ni_{80}Fe_{20}$ in the orthogonal configuration where the initial state is in-plane, namely y-axis. The electrical current density was varied from 0.5×10^7 A/cm^2 to 6.0×10^7 A/cm^2.

6. Ni (y axis)

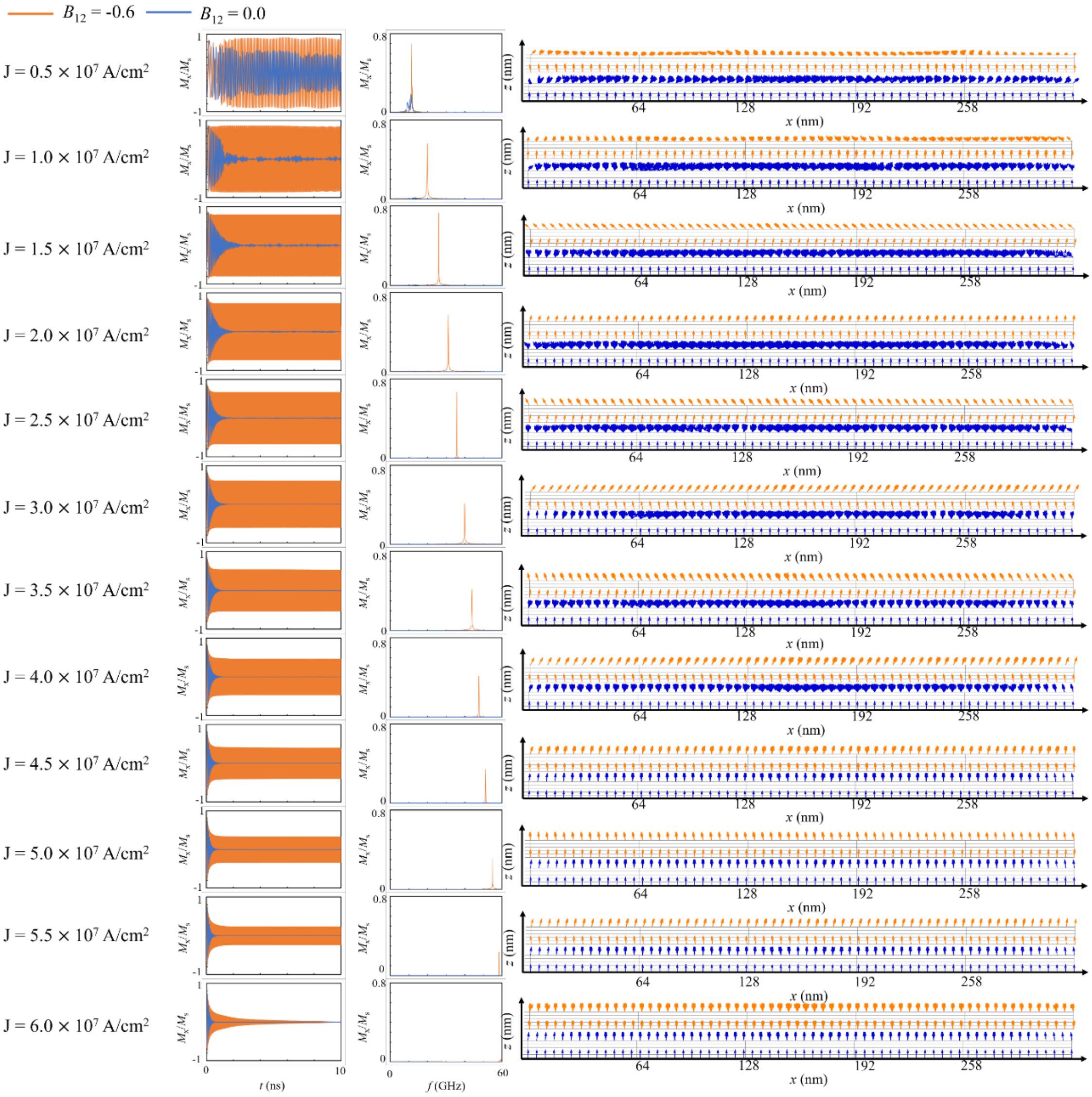

Fig. S6 STO performances for the top layer Ni in the orthogonal configuration where the initial state is in-plane, namely y-axis. The electrical current density was varied from 0.5×10^7 A/cm^2 to 6.0×10^7 A/cm^2.